

Explaining Visual Biases as Words by Generating Captions

Younghyun Kim^{*1} Sangwoo Mo^{*1} Minkyu Kim¹ Kyungmin Lee¹ Jaeho Lee² Jinwoo Shin¹

Abstract

We aim to diagnose the potential biases in image classifiers. To this end, prior works manually labeled biased attributes or visualized biased features, which need high annotation costs or are often ambiguous to interpret. Instead, we leverage two types (generative and discriminative) of pre-trained vision-language models to describe the visual bias as a word. Specifically, we propose *bias-to-text* (B2T), which generates captions of the mispredicted images using a pre-trained captioning model to extract the common keywords that may describe visual biases. Then, we categorize the bias type as spurious correlation or majority bias by checking if it is specific or agnostic to the class, based on the similarity of class-wise mispredicted images and the keyword upon a pre-trained vision-language joint embedding space, e.g., CLIP. We demonstrate that the proposed simple and intuitive scheme can recover well-known gender and background biases, and discover novel ones in real-world datasets. Moreover, we utilize B2T to compare the classifiers using different architectures or training methods. Finally, we show that one can obtain debiased classifiers using the B2T bias keywords and CLIP, in both zero-shot and full-shot manners, without using any human annotation on the bias.¹

1. Introduction

Identifying and removing potential biases in models (i.e., model failure incurred by a specific data attribute or group) is an essential problem in deploying machine learning systems. For example, assume a gender classifier has a wrong stereotype that one who likes to play sports would like to be a male; then it can raise a severe fairness issue (Mehrabian et al., 2021). In addition, the bias in a model hurts generalization performance as the learned bias may not be applied

^{*}Equal contribution ¹KAIST ²POSTECH. Correspondence to: Younghyun Kim <younghyun.kim@kaist.ac.kr>, Sangwoo Mo <swmo@kaist.ac.kr>.

Preprint. Under review.

¹Code: <https://github.com/alinlab/b2t>

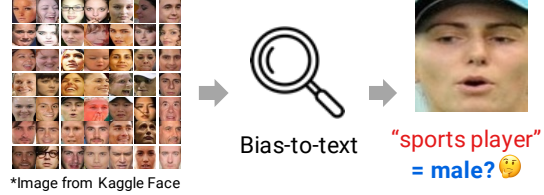


Figure 1: Concept of our proposed bias-to-text (B2T). B2T extracts the common keywords from the captions of mispredicted images, which imply the potential biases in the model. For example, B2T found that “sports player” tends to be mispredicted in the “female” class, implying gender bias in the classifier trained on Kaggle Face (Chauhan, 2020).

to the other situations, e.g., the ratio of female athletes can differ among the social groups (Geirhos et al., 2020). Thus, there were tremendous efforts to recognize biases (Nushi et al., 2018) and debias models (Sagawa et al., 2020).

Despite the efforts, discovering biases in image classifiers is challenging since explaining the reason for the failures of image classifiers is nontrivial. To this end, prior works manually labeled biased attributes (Idrissi et al., 2022) or visualized biased features (Singla et al., 2021), which require high annotation costs or are often ambiguous to interpret. Indeed, the visualization only gives an intuition for the failure of a single image, and aggregating the information to diagnose the bias requires a careful analysis from human experts. On the contrary, analyzing the biases in tabular and language data is relatively easy as the table items and words are more human-interpretable (Ribeiro et al., 2020).

Recently, vision-language models have shown remarkable success in various applications, including zero-shot classification (Radford et al., 2021), caption generation (Mokady et al., 2021), or output manipulation through prompt guidance (Patashnik et al., 2021). Inspired by this advent, we aim to leverage the pre-trained vision-language models to describe visual biases as interpretable words.

We propose *bias-to-text* (B2T), which discovers the biases in image classifiers by text description. Our core idea is to generate captions of the mispredicted images, which represent the bias in the model. For example, the mispredicted images of a biased gender classifier may contain female sports players. Here, we leverage the pre-trained vision-language models, e.g., ClipCap (Mokady et al., 2021) cap-

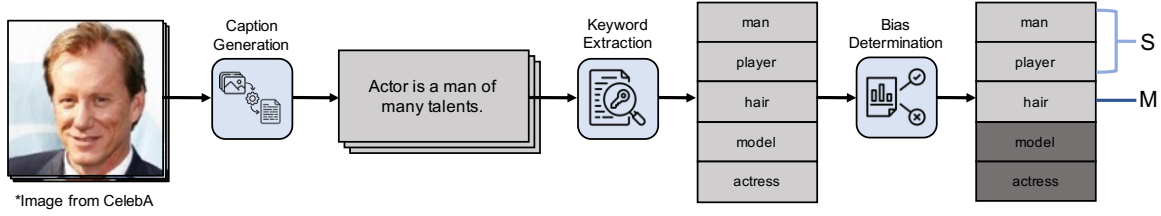


Figure 2: Visual illustration of the B2T framework. First, we generate the captions of the mispredicted (potentially biased) samples. Then, we extract the common keywords in the mispredicted samples. Finally, we determine the bias type, e.g., spurious correlation (S) or majority bias (M), based on a bias-likeness score defined by CLIP embedding similarity.

tioning model built upon the CLIP (Radford et al., 2021) embedding. We then extract the common keywords from the captions as the candidates for the biases.

We further classify the bias type based on the bias-likeness score, which measures the similarity between the keyword and the mispredicted images in the CLIP embedding space. We check if the keyword is a bias for each class based on the score on class-wise mispredicted images. Then, we call the keyword a spurious correlation if it is bias only for a specific class, e.g., “sports player” for females. In contrast, we call the keyword a majority bias if it is bias for all classes, e.g., “young” ones are hard to classify for all genders.

We demonstrate various applications of B2T. In Section 4, we discover the biases in various datasets:

- Recover the well-known biases: find the bias “man” for the “blond” class implying gender bias in CelebA (Liu et al., 2015), “forest” and “ocean” implying background bias in Waterbirds (Sagawa et al., 2020), and “drawing” in ImageNet-R (Hendrycks et al., 2021) and “snow” in ImageNet-C (Hendrycks & Dietterich, 2019) implying that the model fails in natural corruptions.
- Discover the novel biases: find the bias “sports player” for the “female” class implying gender bias in Kaggle Face (Chauhan, 2020), in addition to the geographic and contextual biases in Dollar Street (Rojas et al., 2022) and ImageNet (Deng et al., 2009), e.g., the classifier thinks a “toilet tissue” torn by a “cat” is paper towel since cats are more likely to be at a kitchen than a toilet.

In Section 5, we study the behaviors of various classifiers using different architectures and training methods with B2T. Here, we observed that ViT (Dosovitskiy et al., 2020) better understands the global contexts and is more robust to fine-grained classes than ResNet (He et al., 2016). In addition, debiased models (Sagawa et al., 2020, GDRO) provide more bias-neutral words than biased models (ERM), indicating that B2T can evaluate the biased-ness of the models.

In Section 6, we further demonstrate that one can obtain debiased classifiers using B2T keywords. To this end, we first infer the group (or bias) labels using a CLIP zero-shot classifier by prompting with B2T keywords. We then apply the GDRO (Sagawa et al., 2020) algorithm to train a

debiased classifier using the obtained group labels, which outperforms the baselines. Moreover, we show that B2T can improve the robustness of a CLIP zero-shot classifier by simply augmenting prompts with B2T keywords.

2. Related work

Detailed discussion on related works is in Appendix G.

Bias and fairness. Bias in datasets and models has been a long-lasting issue in machine learning (Torralba & Efros, 2011), and numerous types of biases were investigated. *Majority bias* occurs from an imbalance in dataset (Johnson & Khoshgoftaar, 2019), often amplified by the model. Here, people aim to balance the performance in major and minor groups, which is also related to the fairness issue (Mehrabian et al., 2021). Another type is *spurious correlation*, i.e., a model makes a decision based on spurious features instead of core features (Sagawa et al., 2020). B2T determines the bias type by checking if the bias is class-specific or not.

Bias discovery. Prior works mostly labeled biased attributes by crowdsourcing (Idrissi et al., 2022) or visualized biased features (Singla et al., 2021). Instead, we propose to describe the visual biases with language. Some recent works use vision-language models to analyze the model failures by detecting outliers in the visual embedding (Eyuboglu et al., 2022; Jain et al., 2022a). In contrast, we directly generate descriptive captions from images instead of embeddings, and could find multiple and fine-grained biases. In addition, B2T has several benefits, e.g., categorizing bias types.

Debiasing classifier. Distributionally robust optimization (Rahimian & Mehrotra, 2019, DRO) is a popular method to train a debiased classifier. However, DRO requires expensive sample-wise group labels regarding the bias (Sagawa et al., 2020). Some works addressed this issue by inferring the group labels (Nam et al., 2020; Liu et al., 2021). We show that B2T can be used to estimate the group labels by leveraging a pre-trained vision-language model, which leads to more accurate bias group estimation and better debiased training than prior competitors (see Section 6).

Vision-language models. B2T is heavily inspired by the success of vision-language models (Radford et al., 2021), particularly captioning models (Mokady et al., 2021).

Table 1: Candidates of bias keywords for (a) CelebA blond, (b) waterbird, and (c) landbird classes. Score denotes the bias-likeness score in Eq. (1), Acc. denotes the subgroup accuracy for the given bias keyword, and Bias denotes the type of bias. Words with the highest bias-likeness scores tend to be a spurious correlation (S, class-specific), and the next highest ones tend to be a majority bias (M, class-agnostic). For example, “man” is a spurious correlation to the class “blond” as “blond man” is rare in CelebA. In contrast, “hair” is a majority bias as it indicates the images with unique hairstyles (e.g., partially dyed), which are rare in both “blond” and “not blond” classes. On the other hand, waterbird and landbird only have spurious correlations (land-related words for waterbird and vice versa) and no common majority biases.

(a) CelebA blond (base acc.: 86.0)				(b) Waterbird (base acc.: 75.6)				(c) Landbird (base acc.: 89.9)			
	Score	Acc.	Bias		Score	Acc.	Bias		Score	Acc.	Bias
man	1.22	38.2	S	forest	2.12	61.5	S	ocean	3.41	44.4	S
player	0.42	27.8	S	woods	1.94	62.5	S	beach	2.83	74.7	S
person	0.17	79.8	S	tree	1.45	41.7	S	surfer	2.73	55.6	S
artist	0.16	69.6	S	branch	1.20	35.7	S	boat	2.16	64.7	S
comedy	0.16	88.2	S	prey	0.20	70.0	S	dock	1.56	75.0	S
film	0.13	88.3	S	wild	0.19	75.0	S	water	1.38	75.0	S
actor	0.08	88.2	S	bird of prey	-0.03	66.7	-	lake	1.17	80.0	S
face	0.06	88.5	S	species	-0.05	74.2	-	rocks	1.02	76.5	S
love	0.06	91.3	M	area	-0.09	0.0	-	sunset	0.88	70.0	S
clothing	0.05	93.5	M	biological species	-0.11	74.2	-	kite	0.67	64.6	S
outfit	0.05	93.5	M	bird in flight	-0.27	50.0	-	sky	0.28	84.2	S
hair	0.02	91.2	M	biological	-0.28	74.2	-	flight	0.23	62.5	S
style	0.00	92.2	-	bird	-0.36	62.5	-	flies	-0.17	73.3	-
weight	-0.06	93.6	-	person	-0.41	81.3	-	person	-0.38	86.9	-
clothing style	-0.08	93.5	-	bird flying	-0.42	75.0	-	pond	-0.47	87.0	-
model	-0.19	95.5	-	eagle	-0.69	95.5	-	biological species	-0.48	95.5	-
premiere	-0.52	89.1	-	bald	-0.69	60.0	-	biological	-0.55	93.4	-
premiere of comedy	-0.63	86.2	-	snow	-0.80	66.7	-	species in flight	-0.92	44.4	-
model and actress	-1.00	82.7	-	great bird	-0.80	0.0	-	species	-0.97	93.4	-
actress	-1.28	83.3	-	large bird	-1.05	50.0	-	bird	-1.64	93.8	-

3. B2T: Bias discovery by text description

We aim to discover the *bias* of a classifier, an attribute in data that incurs the failure of the prediction. Precisely, given a classification problem to predict a label $y \in \mathcal{Y}$ of data $x \in \mathcal{X}$, we call an attribute $a \in \mathcal{A}$ is bias if data with attribute a tend to be misclassified, i.e., their subgroup accuracy is lower than the average.² Our idea is to interpret the reason for the failures of wrong samples with language.

Our bias-to-text (B2T) framework discovers biases following the three-step procedure, as illustrated in Figure 2:

1. Generate the captions of mispredicted samples. We use ClipCap (Mokady et al., 2021) captioning model.
2. Extract the common keywords from the captions. We use YAKE (Campos et al., 2020) algorithm.
3. Confirm the bias type based on the bias-likeness score. The detailed procedure is in the following paragraph.

Bias-likeness score. Captioning models only allow us to check if an image has an attribute (i.e., the caption has the keyword), as they only generate some representative words. Thus, we double-check the relations between words and images using their similarities; bias keywords should be closer to the wrong samples than the correct ones. Specifically, we

²We only consider the subgroup type of biases. See Appendix F for a broader discussion on different bias types.

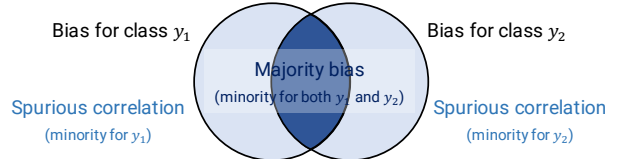


Figure 3: Categorization of bias types.



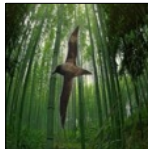



use CLIP (Radford et al., 2021) to define the bias-likeness score of a word a given the dataset \mathcal{D} :

$$s(a; \mathcal{D}) := \text{sim}(a, \mathcal{D}_{\text{wrong}}) - \text{sim}(a, \mathcal{D}_{\text{correct}}) \quad (1)$$

where $\mathcal{D}_{\text{correct}}, \mathcal{D}_{\text{wrong}} \subset \mathcal{D}$ denote the correct and wrong samples, and $\text{sim}(a, \mathcal{D})$ is the similarity between the word a and dataset \mathcal{D} , averaging the cosine similarities between word embedding $f_{\text{text}}(a)$ and image embeddings $f_{\text{image}}(x)$ for $x \in \mathcal{D}$, i.e., $\text{sim}(a, \mathcal{D}) := \frac{1}{|\mathcal{D}|} \sum_{x \in \mathcal{D}} f_{\text{image}}(x) \cdot f_{\text{text}}(a)$, where the embeddings are normalized to a norm of one. We call a word a bias if it has a positive bias-likeness score. The words with high scores tend to be more minor, while low scores are more major. We also define the subgroup for a as the samples which contain the word a in their captions. Minority words tend to have lower subgroup accuracies.

Now we further categorize the bias types using the bias-likeness score. Concretely, we say an attribute a is a *spurious correlation* for a class y if it is a minority for y but not for others. For example, “man” is a spurious correlation for the “blond” class since it is a minority for blonds but not for

Explaining Visual Biases as Words by Generating Captions

(a) CelebA Blond					(b) Waterbirds			
Keyword	Man		Hair		Forest	Woods	Ocean	Beach
Samples								
Actual	blond	blond	not blond	blond	waterbird	waterbird	landbird	landbird
Pred.	not blond	not blond	blond	not blond	landbird	landbird	waterbird	waterbird
Caption	actor as a young man.	person, a man with a beard.	i want my hair like this!	i want to do this to my hair.	a bird in the forest.	a bird in the woods.	a bird in the ocean.	a bird on the beach.


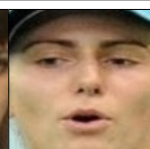






(c) Kaggle Face					(d) Dollar Street			
Keyword	Shocked	Player	Girl		-	Cave	-	Fire
Samples								
Actual	female	female	male	male	wardrobe	wardrobe	stove	stove
Pred.	male	male	female	female	wardrobe	poncho	stove	caldron
Caption	person, who was the first person to be evicted from the house, said she was shocked by the abuse.	person was the first player to be named person.	the girl's face is a bit of a mess.	person, pictured with her mother, was a very shy girl.	the back of the wardrobe.	the cave is full of surprises.	a stove for the kitchen.	a fire in the kitchen.
					Country (Income)			
					Romania (\$6256/month)	Tanzania (\$32/month)	United States (\$855/month)	Togo (\$321/month)

Figure 4: Visual examples of mispredicted samples, their captions, and the bias keywords inferred by B2T on (a) CelebA blond, (b) Waterbirds, (c) Kaggle Face, and (d) Dollar Street datasets. First, B2T could recover the known biases (spurious correlations) such as “man” for CelebA blond, “forest” for waterbird, and “ocean” for landbird classes. In addition, B2T found a novel bias “hair” in CelebA, indicating the images with unique hairstyles (e.g., partially dyed). The “hair” bias appeared in both blond and not blond classes and was determined as a majority bias, as discussed in Table 1. Finally, B2T discovered novel spurious correlations. In Kaggle Face, we found “shocked” and (sports) “player” for females and “girl” for males. It implies that the classifier thinks people not smiling or doing sports are less to be females, and unisex or young people (possibly age bias) are less to be males. In Dollar Street, we found the bias keywords “cave” for wardrobe and “fire” for stove classes, explaining the wrong prediction of objects from low-income countries.

non-blonds. On the other hand, we say an attribute a is a *majority bias* if it is a minority for all classes. For example, people with unique hairstyles are rare for both blonds and non-blonds, and the classifier fails regardless of the class. Figure 3 visualizes the concept of two biases. We determine the bias type by computing the bias-likeness scores for the class-wise subsets $\mathcal{D}^y = \{(x', y') \in \mathcal{D} \mid y' = y\}$. Here, we determine the bias type of a as:

Spurious correlation: $s(a; \mathcal{D}^{y_1}) > 0, s(a; \mathcal{D}^{y_2}) < 0$

Majority bias: $s(a; \mathcal{D}^{y_1}) > 0, s(a; \mathcal{D}^{y_2}) > 0$

where y_1 is target class and y_2 are other classes. We compute the class-wise bias-likeness score if not specified.




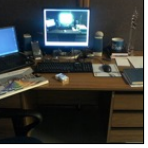



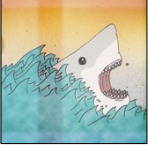
Choice of captioning models. Different captioning models give reliable B2T results as shown in Appendix B. Yet, the user should be aware that the captioning model itself can be biased, as discussed in the limitations in Appendix H.

4. Case studies

4.1. Can B2T identify the well-known biases?

We check the bias discovery ability of B2T. First, we apply B2T to CelebA (Liu et al., 2015) and Waterbirds (Sagawa et al., 2020) datasets to check if B2T identifies the well-known gender and background biases. Then, we apply B2T to Kaggle Face (Chauhan, 2020) and Dollar Street (Rojas et al., 2022) datasets to discover novel biases.

Explaining Visual Biases as Words by Generating Captions

	(a) ImageNet				(b) ImageNet-R			
Keyword	Cat	Beer	Street	Office	Illustration		Drawing	
Samples								
Actual	toilet tissue	beaker	plastic bag	notebook	backpack	hen	bald eagle	white shark
Pred.	paper towel	beer glass	cowboy hat	desk	maze	comic book	isopod	envelope
Caption	cat playing with a piece of paper.	the beer poured into a glass.	police officers patrol the streets.	my desk in the office.	hand drawn illustration of a backpack.	illustration of a rooster on white background.	a drawing of a bald eagle.	a drawing of a shark attacking a white shark.

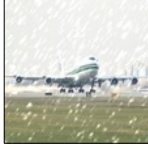







	(c) ImageNet-C snow				(d) ImageNet-C frost			
Keyword	Snow		Rain		Window		Glass	
Samples								
Actual	airliner	airliner	mosquito net	mosquito net	American egret	American egret	green snake	green snake
Pred.	damselfly	airliner	shower cap	mosquito net	quill	American egret	rock beauty	green snake
Caption	airliner in the snow, photo.	airliner lands on the runway.	the umbrella in the rain.	the baby in the tent.	a bird on a frozen window.	biological species in flight over the sea.	a frog in a glass of water.	a green frog in the jungle.

Figure 5: Visual examples of mispredicted samples, their captions, and the bias keywords inferred by B2T on (a) ImageNet, (b) ImageNet-R, (c) ImageNet-C snow, and (d) ImageNet-C frost datasets. In ImageNet, B2T discovered novel spurious correlations between objects in scene images, such as “toilet tissue” torn by a “cat” is predicted as “paper towel.” For ImageNet variants, B2T recovered the natural corruptions such as “illustration” and “drawing” in ImageNet-R and “snow” in ImageNet-C snow. In addition, B2T discovered novel biases such as “window” for ImageNet-C frost. It suggests a new natural corruption “behind window” which visually resembles the frosted images. Lastly, B2T discovered fine-grained bias keywords such as “hand drawn” or “vector art” for ImageNet-R, as shown in Table 15 in Appendix C.

Table 1 presents the candidates of bias keywords of CelebA and Waterbirds. We focus on the visual examples and their implications in the main paper. See Appendix C for the full lists of bias keywords and Appendix D for additional visual examples. See Appendix A for implementation details.

CelebA blond. CelebA (Liu et al., 2015) contains facial images of celebrities. Following Sagawa et al. (2020), we consider the task of classifying “blond” and “not blond” hair colors, where the class “blond” is spuriously correlated with an attribute “male,” i.e., most blonds are females. We apply B2T to the validation set of CelebA blond using the ERM classifier released by Sagawa et al. (2020).

Table 1a presents the bias keywords for CelebA blond class. The word “man” has the highest bias-likeness score, indicating that gender bias is severe for CelebA blond. This gender bias is predicted as a spurious correlation specific to the blond class. In contrast, the word “actress” implies that “woman” has the lowest bias-likeness score.

On the other hand, the words with mid-high bias-likeness scores such as “hair” and “outfit” are predicted as majority biases. These words appear in the captions when the images have unique hairstyles (or outfits), and thus are rare for both blond and not blond classes. Figure 4a visualizes the examples of “man” and “hair” bias keywords.

Waterbirds. Waterbirds (Sagawa et al., 2020) contains images of waterbirds and landbirds. Waterbirds are mostly in water backgrounds but rarely in land backgrounds, i.e., the class “waterbird” is spuriously correlated with a background bias “land” (and vice versa for landbirds). We apply B2T to the validation set of Waterbirds using the ERM classifier released by Sagawa et al. (2020).

Table 1b and 1c present the bias keywords for waterbird and landbird classes. Unlike CelebA blond, all bias keywords are predicted as spurious correlations, i.e., two groups are disjointed and no common majority bias exists. To be specific, B2T predicted land-related words such as “forest”

Explaining Visual Biases as Words by Generating Captions



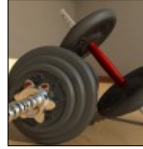





Class	toilet tissue		dumbbell		shopping basket		crayfish	
Samples								
Pred. by ResNet	toilet tissue	paper towel	dumbbell	horizontal bar	shopping basket	grocery store	crayfish	rock crab
Pred. by ViT	toilet tissue	toilet tissue	dumbbell	dumbbell	shopping basket	shopping basket	crayfish	crayfish
Keyword	-	Cat	-	Work out	-	Supermarket	-	Crab
Caption	a toilet paper roll on a white background.	cat playing with a paper cup.	a set of dumbbells with weights.	person works out in the gym.	a basket full of food.	woman shopping in a supermarket.	a lobster is seen in the grass.	a crab in the water.

Figure 6: Comparison of ResNet and ViT architectures using B2T. We train and evaluate the models on ImageNet, and report the predicted labels from both models and B2T results from ResNet. We observed that ViT better understands the global contexts and is more robust to fine-grained classes than ResNet. For example, ResNet fails in complex images whose B2T keywords depict abstract contexts such as “work out” and “supermarket.” ViT successfully predicts those complex scenes, fixes the “cat” bias in “toilet tissue,” and recognizes fine-grained “crayfish” instead of lumping it as “crab.”

and “woods” for waterbird, and water-related words such as “ocean” and “beach” for landbird. Recall that B2T found the fine-grained bias keywords beyond “water” and “land.” Figure 4b visualizes the examples.

Kaggle Face. Kaggle Face (Chauhan, 2020) contains face images of males and females. We train a gender classifier on the training split and apply B2T to the validation split.

We discovered several unknown biases that affect the gender classifier (full list of bias keywords is in Table 12 in Appendix C). We highlight some examples in Figure 4c. For females, we discovered spurious correlations “shocked” and “player.” The word “shocked” implies the stereotype that women smile more than men (Briton & Hall, 1995). The word “player” implies the bias that sports are the men’s league (Meier, 2000). For males, we discovered a spurious correlation “girl,” suggesting the potential age bias.

Dollar Street. Dollar Street (Rojas et al., 2022) contains object images from countries with different income levels. Prior works revealed that classifiers perform worse for objects from low-income countries (De Vries et al., 2019). We aim to take a deeper look at this geographic bias. We apply B2T to the validation set of Dollar Street using the ImageNet (Deng et al., 2009) supervised classifier.

Figure 4d visualizes the examples. The classifier predicted the correct labels for the objects from high-income countries but failed for low-income countries. Here, B2T discovered the bias keywords “cave” for “wardrobe” and “fire” for “stove” classes; wardrobes from low-income countries are often in dark places that look like caves, and stoves from low-income countries often have a traditional design using fire. It makes the classifier confuse the context and mislead

the prediction. See Appendix D for additional results, e.g., bias “bucket” for classes “plate rack” and “toilet tissue.”

4.2. Discovering biases in ImageNet variants

We apply B2T to a more challenging scenario: discovering biases in ImageNet (Deng et al., 2009). Since ImageNet has many classes, we demonstrate the class-wise examples of the hard classes that the classifier fails the most. We use the supervised ResNet-50 (He et al., 2016) classifier.

We also apply B2T to ImageNet variants containing hard samples with natural corruptions. The corruption can be considered as bias, as it is rare (or does not exist) in the training dataset. Specifically, we evaluate the ImageNet supervised classifier on ImageNet-R (Hendrycks et al., 2021) and ImageNet-C (Hendrycks & Dietterich, 2019). We apply B2T to the union of ImageNet and each variant (not class-wise), since our goal is to identify the failures of the classifier when applied to the uncured real-world data which may contain both natural and corrupted images.

ImageNet. Figure 5a visualizes the examples of ImageNet. We found spurious correlations between objects in the scene. For example, the classifier predicts “toilet tissue” with keyword “cat (playing)” as “paper towel,” as cats are more likely to be at a kitchen than a toilet. Another example, “beaker,” shows that the classifier suffers from the bias of predicting the beakers filled with yellow liquid as “beer.” Finally, B2T suggests the bias keywords “street” and “office” for “plastic bag” and “notebook” classes. It implies that the classifier has difficulty in classifying objects in complex scenes with multiple objects. See Appendix D for more examples.

ImageNet-R. ImageNet-R (rendition) contains artistic images of ImageNet classes. Since the ImageNet classifier is

Table 2: Comparison of ERM and GDRO training using B2T, under (a) CelebA blond, (b) waterbird, and (c) landbird datasets. We present the top 10 bias keywords from ERM in Table 1 and compare the bias-likeness scores of ERM, GDRO, and their gap. We mark \times if GDRO does not find the bias keyword and highlight the score gap of highly-biased words (score > 0.2 for ERM). GDRO finds more bias-neutral results, e.g., “man” and “player” are disappeared in CelebA blond, and bias-likeness scores of highly-biased words are decreased for Waterbirds, e.g., $3.41 \rightarrow 1.98$ for “ocean” in landbird.

(a) CelebA blond				(b) Waterbird				(c) Landbird			
	ERM	GDRO	Gap		ERM	GDRO	Gap		ERM	GDRO	Gap
man	1.22	\times	\times	forest	2.12	1.83	-0.29	ocean	3.41	1.98	-1.43
player	0.42	\times	\times	woods	1.94	1.67	-0.27	beach	2.83	1.39	-1.45
person	0.17	0.05	-0.12	tree	1.45	1.66	+0.21	surfer	2.73	1.55	-1.18
artist	0.16	\times	\times	branch	1.20	1.23	+0.03	boat	2.16	1.14	-1.02
comedy	0.16	\times	\times	prey	0.20	\times	\times	dock	1.56	0.59	-0.97
film	0.13	0.48	+0.32	wild	0.19	\times	\times	water	1.38	0.84	-0.54
actor	0.08	-0.38	-0.40	bird of prey	-0.03	\times	\times	lake	1.17	\times	\times
face	0.06	\times	\times	species	-0.05	0.03	+0.08	rocks	1.02	\times	\times
love	0.06	0.36	+0.30	area	-0.09	0.13	+0.24	sunset	0.88	\times	\times
clothing	0.05	0.16	+0.11	biological species	-0.11	0.08	+0.19	kite	0.67	\times	\times

trained on photo-like images, it fails to predict such artistic images. Figure 5b presents that B2T could identify the artistic styles such as “illustration” and “drawing.” Moreover, B2T gives fine-grained bias keywords such as “hand drawn” or “vector art” as shown in Table 15 in Appendix C.

ImageNet-C. ImageNet-C (corruption) contains noisy images of ImageNet classes. Figure 5c and Figure 5d present examples of “snow” and “frost” corruptions. For the snow corruption, B2T captured the exact keywords “snow” and “rain.” For the frost corruption, B2T captured the keywords “window” and “glass.” Intuitively, the frozen images visually resemble the ones with novel bias, “behind window.”

5. Comparison of different classifiers

We use B2T to compare the behaviors of different classifiers, analyzing their mispredicted images and bias keywords.

5.1. Architectures: ResNet vs. ViT

We compare ResNet (He et al., 2016) and ViT (Dosovitskiy et al., 2020) architectures. Recent studies claim that ViT is more robust than ResNet by better understanding the object shapes (Naseer et al., 2021). We further investigate their behaviors by looking at the B2T keywords. We train and evaluate models on ImageNet, as with Section 4.2.

Figure 6 presents the comparison results. ViT better understands the global contexts and is more robust to fine-grained classes than ResNet. For example, ViT successfully predicts complex images with abstract bias keywords such as “work out” that ResNet fails. We think that the global operation of self-attention helps the model look at the contexts.

5.2. Training methods: ERM vs. GDRO

We compare biased and debiased training methods: empirical risk minimization (ERM) and group distributionally

robust optimization (Sagawa et al., 2020, GDRO). Table 2 compares the B2T results of ERM and GDRO. The full list of bias keywords from GDRO is in Table 16 in Appendix C. GDRO gives more bias-neutral words, e.g., no “man” for CelebA blond, and decreases bias-likeness scores. Thus, one can use B2T to evaluate the biased-ness of models.

We compare other training methods in Appendix E. Multimodal model less captures style-related words, i.e., robust to distribution shifts. Self-supervised model captures similar words to the supervised model although its accuracy is higher, i.e., its qualitative behaviors are unchanged.

6. Debiasing classifiers with B2T

We first show that one can infer the group labels by using CLIP zero-shot classifier by prompting with B2T keywords (Section 6.1), then we train a debiased classifier using the obtained group labels (Section 6.2). Lastly, we show that B2T can improve the robustness of zero-shot classifier by augmenting prompts with B2T bias keywords (Section 6.3). Experimental details are illustrated in Appendix A.3.

6.1. Inferring group labels with B2T keywords

We infer the group (or bias) labels of training samples with the CLIP zero-shot (ZS) classifier. To this end, we create the prompts “a photo of a [group]”³ and find the nearest prompt for an image to assign the group label. Here, choosing the proper words for [group] is critical.

To verify this, we generate prompts using B2T words, e.g., {“forest,” “ocean,” ...} reported in Table 1 for Waterbirds. We refer to it as CLIP ZS w/ B2T prompt. For comparison, we directly use the group names, e.g., {“land,” “wa-

³The exact prompt template depends on the dataset, e.g., we use “a photo of a bird in the [group]” for Waterbirds, where [group] is a bias keyword like forest or ocean.

Table 3: Precision (P), recall (R), and F1-score (F1) of group labels inferred by prior methods and CLIP zero-shot (ZS) classifier, using the group names or B2T for prompts. We **bold** the best values. Ours outperforms the prior methods and the base CLIP ZS using group prompts.

	CelebA blond			Waterbirds		
	P	R	F1	P	R	F1
ERM prediction (Liu et al., 2021)	0.22	0.64	0.33	0.21	0.71	0.33
GEORGE (Sohoni et al., 2020)	0.16	0.83	0.27	0.13	0.74	0.22
CLIP ZS w/ group prompt (Zhang & Ré, 2022)	0.96	0.95	0.96	0.25	0.59	0.35
CLIP ZS w/ B2T prompt (ours)	0.96	0.95	0.96	0.66	0.88	0.76

Table 4: Worst-group and average accuracies (%) of our debiased classifier (GDRO-B2T) and prior works. GT denotes the usage of ground-truth group labels for training. We **bold** the best worst-group accuracy. Ours performs the best.

Method	GT	CelebA blond		Waterbirds	
		Worst	Avg.	Worst	Avg.
ERM	-	47.7±2.1	94.9	62.6±0.3	97.3
LfF (Nam et al., 2020)	-	77.2	85.1	78.0	91.2
GEORGE (Sohoni et al., 2020)	-	54.9±1.9	94.6	76.2±2.0	95.7
JTT (Liu et al., 2021)	-	81.5±1.7	88.1	83.8±1.2	89.3
CNC (Zhang et al., 2022)	-	88.8±0.9	89.9	88.5±0.3	90.9
GDRO-B2T (ours)	-	90.4±0.9	93.2	90.7±0.3	92.1
GDRO (Sagawa et al., 2020)	✓	90.0±1.5	93.3	89.9±1.3	91.5

ter”} as in Zhang & Ré (2022), which we call CLIP ZS w/ group prompt. A detailed list of the prompts is in Table 7 in Appendix A. We also compare with unsupervised bias discovery methods such as “ERM prediction” (Liu et al., 2021), which used the prediction of a biased ERM model, and “GEORGE” (Sohoni et al., 2020), which used Gaussian mixture model on the embedding space.

Table 3 shows the accuracies of predicted group labels from each method. CLIP ZS w/ B2T prompt significantly outperforms the unsupervised bias discovery methods, confirming the effectiveness of B2T in a combination of the pre-trained vision-language model. Also, using the fine-grained group words from B2T is crucial; CLIP ZS w/ group prompt performs poorly on Waterbirds. Both work well on CelebA blond as they mostly rely on the word “man.”

6.2. Training debiased classifiers with B2T group labels

Given the group labels acquired in Subsection 6.1, we train a debiased classifier by applying GDRO (Sagawa et al., 2020), where we refer to it as GDRO-B2T. We compare GDRO-B2T (ours) with various baselines, including empirical risk minimization (ERM), GDRO using the ground-truth (GT) group labels, and debiased training methods that infer the group labels in an unsupervised manner: LfF (Nam et al., 2020), GEORGE (Sohoni et al., 2020), JTT (Liu et al., 2021), and CNC (Zhang et al., 2022). The values except GDRO and GDRO-B2T are excerpted from CNC paper.

Table 4 presents the worst-group and average accuracies. GDRO-B2T (ours) outperforms the prior methods that infer

Table 5: Worst-group and average accuracies (%) of CLIP zero-shot classifier (ZS) using the base prompt or augmented ones: using the base group names (“group”) or B2T words with positive (“B2T-pos”) or negative (“B2T-neg”) bias-likeness scores. We **bold** the best worst-group accuracy. “B2T-pos” highly improves worst-group accuracy, but “group” less helps and “B2T-neg” even harms.

	CelebA blond		Waterbirds	
	Worst	Avg.	Worst	Avg.
CLIP ZS	76.2	85.2	50.3	72.7
+ Group prompt (Zhang & Ré, 2022)	76.7	87.0	53.7	78.0
+ B2T-neg prompt	72.9	88.0	45.4	70.8
+ B2T-pos prompt (ours)	80.0	87.2	61.7	76.9

the group labels in an unsupervised manner, verifying the effect of B2T which leverages pre-trained vision-language models. GDRO-B2T also surpasses GDRO using GT labels, perhaps due to the noises in GT group annotations.

6.3. Debiasing zero-shot classifiers with B2T prompts

Lastly, we debias the zero-shot (ZS) classifiers such as CLIP by augmenting B2T words to the prompts. Recall that the original CLIP uses a prompt template “a photo of a [class]”. We modify the prompt as “a photo of a [class] in the [group]” by augmenting a group word at the suffix. Here, we average the text embeddings from the prompts of all groups and find the nearest one to the image embedding to assign the class label.

We compare different sets of group words to verify their importance. Specifically, we use B2T words with positive or negative bias-likeness scores, called B2T-pos and B2T-neg, respectively. For example, we use “ocean” for B2T-pos and “bird” for B2T-neg for Waterbirds, as shown in Table 1. Intuitively, B2T-pos words are more spuriously correlated with the class, being more helpful for recognizing the minor group. A detailed list of the prompts is in Table 8 in Appendix A. We also tested the base group names (e.g., “water”) as in Zhang & Ré (2022), following Section 6.1.

Table 5 presents the worst-group and average accuracies of CLIP ZS classifiers using the base prompt or augmented ones with group words. B2T-pos group words improves both worst-group and average accuracies. In contrast, base group names are less helpful and B2T-neg group words even degrade worst-group accuracy. B2T-augmented prompts improve the fairness of ZS classifiers without fine-tuning.

7. Conclusion

We propose *bias-to-text* (B2T), which discovers the biases in image classifiers using vision-language models. We present various applications of B2T, discovering novel biases in real-world datasets, analyzing behaviors of different classifiers, and debiasing classifiers. We hope B2T could help future bias research, as discussed in Appendix H.

References

- Adebayo, J., Gilmer, J., Muelly, M., Goodfellow, I., Hardt, M., and Kim, B. Sanity checks for saliency maps. In *Neural Information Processing Systems*, 2018.
- Agarwal, S., Krueger, G., Clark, J., Radford, A., Kim, J. W., and Brundage, M. Evaluating clip: towards characterization of broader capabilities and downstream implications. *arXiv preprint arXiv:2108.02818*, 2021.
- Arjovsky, M., Bottou, L., Gulrajani, I., and Lopez-Paz, D. Invariant risk minimization. *arXiv preprint arXiv:1907.02893*, 2019.
- Bahng, H., Chun, S., Yun, S., Choo, J., and Oh, S. J. Learning de-biased representations with biased representations. In *International Conference on Machine Learning*, 2020.
- Bao, Y. and Barzilay, R. Learning to split for automatic bias detection. *arXiv preprint arXiv:2204.13749*, 2022.
- Bolukbasi, T., Chang, K.-W., Zou, J. Y., Saligrama, V., and Kalai, A. T. Man is to computer programmer as woman is to homemaker? debiasing word embeddings. In *Neural Information Processing Systems*, 2016.
- Bommasani, R., Hudson, D. A., Adeli, E., Altman, R., Arora, S., von Arx, S., Bernstein, M. S., Bohg, J., Bosse-lut, A., Brunskill, E., et al. On the opportunities and risks of foundation models. *arXiv preprint arXiv:2108.07258*, 2021.
- Briton, N. J. and Hall, J. A. Gender-based expectancies and observer judgments of smiling. *Journal of Nonverbal Behavior*, 19(1):49–65, 1995.
- Campos, R., Mangaravite, V., Pasquali, A., Jorge, A., Nunes, C., and Jatowt, A. Yake! keyword extraction from single documents using multiple local features. *Information Sciences*, 509:257–289, 2020.
- Caron, M., Touvron, H., Misra, I., Jégou, H., Mairal, J., Bojanowski, P., and Joulin, A. Emerging properties in self-supervised vision transformers. In *International Conference on Computer Vision*, 2021.
- Chauhan, A. Gender classification dataset. <https://www.kaggle.com/datasets/cashutosh/gender-classification-dataset>, 2020.
- Christie, G., Fendley, N., Wilson, J., and Mukherjee, R. Functional map of the world. In *Conference on Computer Vision and Pattern Recognition*, 2018.
- Chung, Y., Kraska, T., Polyzotis, N., Tae, K. H., and Whang, S. E. Slice finder: Automated data slicing for model validation. In *International Conference on Data Engineering*, 2019.
- Creager, E., Jacobsen, J.-H., and Zemel, R. Environment inference for invariant learning. In *International Conference on Machine Learning*, 2021.
- De Vries, T., Misra, I., Wang, C., and Van der Maaten, L. Does object recognition work for everyone? In *Conference on Computer Vision and Pattern Recognition*, 2019.
- Deng, J., Dong, W., Socher, R., Li, L.-J., Li, K., and Fei-Fei, L. Imagenet: A large-scale hierarchical image database. In *Conference on Computer Vision and Pattern Recognition*, 2009.
- Desai, K. and Johnson, J. Virtex: Learning visual representations from textual annotations. In *Conference on Computer Vision and Pattern Recognition*, 2021.
- Dosovitskiy, A., Beyer, L., Kolesnikov, A., Weissenborn, D., Zhai, X., Unterthiner, T., Dehghani, M., Minderer, M., Heigold, G., Gelly, S., et al. An image is worth 16x16 words: Transformers for image recognition at scale. In *International Conference on Learning Representations*, 2020.
- Engstrom, L., Ilyas, A., Santurkar, S., Tsipras, D., Tran, B., and Madry, A. Adversarial robustness as a prior for learned representations. *arXiv preprint arXiv:1906.00945*, 2019.
- Esser, P., Rombach, R., and Ommer, B. Taming transformers for high-resolution image synthesis. In *Conference on Computer Vision and Pattern Recognition*, 2021.
- Eyuboglu, S., Varma, M., Saab, K., Delbrouck, J.-B., Lee-Messer, C., Dunnmon, J., Zou, J., and Ré, C. Domino: Discovering systematic errors with cross-modal embeddings. In *International Conference on Learning Representations*, 2022.
- Fang, A., Ilharco, G., Wortsman, M., Wan, Y., Shankar, V., Dave, A., and Schmidt, L. Data determines distributional robustness in contrastive language image pre-training (clip). *arXiv preprint arXiv:2205.01397*, 2022.
- Geirhos, R., Rubisch, P., Michaelis, C., Bethge, M., Wichmann, F. A., and Brendel, W. Imagenet-trained cnns are biased towards texture; increasing shape bias improves accuracy and robustness. In *International Conference on Learning Representations*, 2019.
- Geirhos, R., Jacobsen, J.-H., Michaelis, C., Zemel, R., Brendel, W., Bethge, M., and Wichmann, F. A. Shortcut learning in deep neural networks. *Nature Machine Intelligence*, 2(11):665–673, 2020.
- He, K., Zhang, X., Ren, S., and Sun, J. Deep residual learning for image recognition. In *Conference on Computer Vision and Pattern Recognition*, 2016.

- He, K., Chen, X., Xie, S., Li, Y., Dollár, P., and Girshick, R. Masked autoencoders are scalable vision learners. In *Conference on Computer Vision and Pattern Recognition*, 2022.
- Hendricks, L. A., Burns, K., Saenko, K., Darrell, T., and Rohrbach, A. Women also snowboard: Overcoming bias in captioning models. In *European Conference on Computer Vision*, 2018.
- Hendrycks, D. and Dietterich, T. Benchmarking neural network robustness to common corruptions and perturbations. In *International Conference on Learning Representations*, 2019.
- Hendrycks, D., Basart, S., Mu, N., Kadavath, S., Wang, F., Dorundo, E., Desai, R., Zhu, T., Parajuli, S., Guo, M., et al. The many faces of robustness: A critical analysis of out-of-distribution generalization. In *International Conference on Computer Vision*, 2021.
- Hernandez, E., Schwettmann, S., Bau, D., Bagashvili, T., Torralba, A., and Andreas, J. Natural language descriptions of deep visual features. In *International Conference on Learning Representations*, 2022.
- Idrissi, B. Y., Bouchacourt, D., Balestrieri, R., Evtimov, I., Hazirbas, C., Ballas, N., Vincent, P., Drozdal, M., Lopez-Paz, D., and Ibrahim, M. Imagenet-x: Understanding model mistakes with factor of variation annotations. *arXiv preprint arXiv:2211.01866*, 2022.
- Jain, S., Lawrence, H., Moitra, A., and Madry, A. Distilling model failures as directions in latent space. *arXiv preprint arXiv:2206.14754*, 2022a.
- Jain, S., Salman, H., Wong, E., Zhang, P., Vineet, V., Vemprala, S., and Madry, A. Missingness bias in model debugging. In *International Conference on Learning Representations*, 2022b.
- Jalal, A., Karmalkar, S., Hoffmann, J., Dimakis, A., and Price, E. Fairness for image generation with uncertain sensitive attributes. In *International Conference on Machine Learning*, 2021.
- Johnson, J. M. and Khoshgoftaar, T. M. Survey on deep learning with class imbalance. *Journal of Big Data*, 6(1): 1–54, 2019.
- Karras, T., Aittala, M., Laine, S., Härkönen, E., Hellsten, J., Lehtinen, J., and Aila, T. Alias-free generative adversarial networks. In *Neural Information Processing Systems*, 2021.
- Kim, B., Kim, H., Kim, K., Kim, S., and Kim, J. Learning not to learn: Training deep neural networks with biased data. In *Conference on Computer Vision and Pattern Recognition*, 2019.
- Kim, J., Hur, Y., Park, S., Yang, E., Hwang, S. J., and Shin, J. Distribution aligning refinery of pseudo-label for imbalanced semi-supervised learning. In *Neural Information Processing Systems*, 2020a.
- Kim, J., Jeong, J., and Shin, J. M2m: Imbalanced classification via major-to-minor translation. In *Conference on Computer Vision and Pattern Recognition*, 2020b.
- Kingma, D. P. and Dhariwal, P. Glow: Generative flow with invertible 1x1 convolutions. In *Neural Information Processing Systems*, 2018.
- Koh, P. W., Sagawa, S., Marklund, H., Xie, S. M., Zhang, M., Balsubramani, A., Hu, W., Yasunaga, M., Phillips, R. L., Gao, I., et al. Wilds: A benchmark of in-the-wild distribution shifts. In *International Conference on Machine Learning*, 2021.
- Leclerc, G., Salman, H., Ilyas, A., Vemprala, S., Engstrom, L., Vineet, V., Xiao, K., Zhang, P., Santurkar, S., Yang, G., et al. 3db: A framework for debugging computer vision models. *arXiv preprint arXiv:2106.03805*, 2021.
- Lee, J., Kim, E., Lee, J., Lee, J., and Choo, J. Learning debiased representation via disentangled feature augmentation. In *Neural Information Processing Systems*, 2021.
- Lee, N. T. Detecting racial bias in algorithms and machine learning. *Journal of Information, Communication and Ethics in Society*, 2018.
- Levy, D., Carmon, Y., Duchi, J. C., and Sidford, A. Large-scale methods for distributionally robust optimization. In *Neural Information Processing Systems*, 2020.
- Li, J., Li, D., Xiong, C., and Hoi, S. Blip: Bootstrapping language-image pre-training for unified vision-language understanding and generation. In *International Conference on Machine Learning*, 2022.
- Liu, E. Z., Haghighi, B., Chen, A. S., Raghunathan, A., Koh, P. W., Sagawa, S., Liang, P., and Finn, C. Just train twice: Improving group robustness without training group information. In *International Conference on Machine Learning*, 2021.
- Liu, Z., Luo, P., Wang, X., and Tang, X. Deep learning face attributes in the wild. In *International Conference on Computer Vision*, 2015.
- Lu, J., Batra, D., Parikh, D., and Lee, S. Vilbert: Pretraining task-agnostic visiolinguistic representations for vision-and-language tasks. In *Neural Information Processing Systems*, 2019.
- Mehrabi, N., Morstatter, F., Saxena, N., Lerman, K., and Galstyan, A. A survey on bias and fairness in machine learning. *ACM Computing Surveys*, 54(6):1–35, 2021.

- Meier, M. *Gender equity, sport and development*. Swiss academy for Development, 2000.
- Mitchell, E., Lin, C., Bosselut, A., Finn, C., and Manning, C. D. Fast model editing at scale. In *International Conference on Learning Representations*, 2022.
- Mo, S., Kim, C., Kim, S., Cho, M., and Shin, J. Mining gold samples for conditional gans. In *Neural Information Processing Systems*, 2019.
- Mo, S., Kang, H., Sohn, K., Li, C.-L., and Shin, J. Object-aware contrastive learning for debiased scene representation. In *Neural Information Processing Systems*, 2021.
- Moayeri, M., Wang, W., Singla, S., and Feizi, S. Spuriousity rankings: Sorting data for spurious correlation robustness. *arXiv preprint arXiv:2212.02648*, 2022.
- Mokady, R., Hertz, A., and Bermano, A. H. Clip-cap: Clip prefix for image captioning. *arXiv preprint arXiv:2111.09734*, 2021.
- Molnar, C. *Interpretable machine learning*. 2020.
- Moon, S. J., Mo, S., Lee, K., Lee, J., and Shin, J. Masker: Masked keyword regularization for reliable text classification. In *AAAI Conference on Artificial Intelligence*, 2021.
- Muandet, K., Balduzzi, D., and Schölkopf, B. Domain generalization via invariant feature representation. In *International Conference on Machine Learning*, 2013.
- Nam, J., Cha, H., Ahn, S., Lee, J., and Shin, J. Learning from failure: De-biasing classifier from biased classifier. In *Neural Information Processing Systems*, 2020.
- Nam, J., Kim, J., Lee, J., and Shin, J. Spread spurious attribute: Improving worst-group accuracy with spurious attribute estimation. In *International Conference on Learning Representations*, 2022a.
- Nam, J., Mo, S., Lee, J., and Shin, J. Breaking the spurious causality of conditional generation via fairness intervention with corrective sampling. *arXiv preprint arXiv:2212.02090*, 2022b.
- Naseer, M. M., Ranasinghe, K., Khan, S. H., Hayat, M., Shahbaz Khan, F., and Yang, M.-H. Intriguing properties of vision transformers. *Neural Information Processing Systems*, 2021.
- Nushi, B., Kamar, E., and Horvitz, E. Towards accountable ai: Hybrid human-machine analyses for characterizing system failure. In *AAAI Conference on Human Computation and Crowdsourcing*, 2018.
- Olah, C., Mordvintsev, A., and Schubert, L. Feature visualization. *Distill*, 2017. doi: 10.23915/distill.00007. <https://distill.pub/2017/feature-visualization>.
- Patashnik, O., Wu, Z., Shechtman, E., Cohen-Or, D., and Lischinski, D. Styleclip: Text-driven manipulation of stylegan imagery. In *International Conference on Computer Vision*, 2021.
- Plumb, G., Ribeiro, M. T., and Talwalkar, A. Finding and fixing spurious patterns with explanations. *Transactions on Machine Learning Research*, 2022.
- Radford, A., Kim, J. W., Hallacy, C., Ramesh, A., Goh, G., Agarwal, S., Sastry, G., Askell, A., Mishkin, P., Clark, J., et al. Learning transferable visual models from natural language supervision. In *International Conference on Machine Learning*, 2021.
- Rahimian, H. and Mehrotra, S. Distributionally robust optimization: A review. *arXiv preprint arXiv:1908.05659*, 2019.
- Rajpurkar, P., Irvin, J., Zhu, K., Yang, B., Mehta, H., Duan, T., Ding, D., Bagul, A., Langlotz, C., Shpanskaya, K., et al. Chexnet: Radiologist-level pneumonia detection on chest x-rays with deep learning. *arXiv preprint arXiv:1711.05225*, 2017.
- Ramesh, A., Pavlov, M., Goh, G., Gray, S., Voss, C., Radford, A., Chen, M., and Sutskever, I. Zero-shot text-to-image generation. In *International Conference on Machine Learning*, 2021.
- Ribeiro, M. T., Wu, T., Guestrin, C., and Singh, S. Beyond accuracy: Behavioral testing of nlp models with checklist. In *Annual Conference of the Association for Computational Linguistics*, 2020.
- Roh, Y., Heo, G., and Whang, S. E. A survey on data collection for machine learning: a big data-ai integration perspective. *IEEE Transactions on Knowledge and Data Engineering*, 33(4):1328–1347, 2019.
- Rojas, W. A. G., Damos, S., Kini, K. R., Kanter, D., Reddi, V. J., and Coleman, C. The dollar street dataset: Images representing the geographic and socioeconomic diversity of the world. In *Neural Information Processing Systems Datasets and Benchmarks Track*, 2022.
- Sagawa, S., Koh, P. W., Hashimoto, T. B., and Liang, P. Distributionally robust neural networks for group shifts: On the importance of regularization for worst-case generalization. In *International Conference on Learning Representations*, 2020.

- Santurkar, S., Tsipras, D., Elango, M., Bau, D., Torralba, A., and Madry, A. Editing a classifier by rewriting its prediction rules. In *Neural Information Processing Systems*, 2021.
- Selvaraju, R. R., Cogswell, M., Das, A., Vedantam, R., Parikh, D., and Batra, D. Grad-cam: Visual explanations from deep networks via gradient-based localization. In *International Conference on Computer Vision*, 2017.
- Shah, H., Park, S. M., Ilyas, A., and Madry, A. Modeldiff: A framework for comparing learning algorithms. *arXiv preprint arXiv:2211.12491*, 2022.
- Sharma, P., Ding, N., Goodman, S., and Soricut, R. Conceptual captions: A cleaned, hypernymed, image alt-text dataset for automatic image captioning. In *Annual Conference of the Association for Computational Linguistics*, 2018.
- Singla, S., Nushi, B., Shah, S., Kamar, E., and Horvitz, E. Understanding failures of deep networks via robust feature extraction. In *Conference on Computer Vision and Pattern Recognition*, 2021.
- Singla, S., Chegini, A. M., Moayeri, M., and Feiz, S. Data-centric debugging: mitigating model failures via targeted data collection. *arXiv preprint arXiv:2211.09859*, 2022.
- Sohoni, N., Dunnmon, J., Angus, G., Gu, A., and Ré, C. No subclass left behind: Fine-grained robustness in coarse-grained classification problems. In *Neural Information Processing Systems*, 2020.
- Sohoni, N., Sanjabi, M., Ballas, N., Grover, A., Nie, S., Firooz, H., and Ré, C. Barack: Partially supervised group robustness with guarantees. *arXiv preprint arXiv:2201.00072*, 2021.
- Song, Y., Sohl-Dickstein, J., Kingma, D. P., Kumar, A., Ermon, S., and Poole, B. Score-based generative modeling through stochastic differential equations. In *International Conference on Learning Representations*, 2021.
- Torralba, A. and Efros, A. A. Unbiased look at dataset bias. In *Conference on Computer Vision and Pattern Recognition*, 2011.
- Vahdat, A. and Kautz, J. Nvae: A deep hierarchical variational autoencoder. In *Neural Information Processing Systems*, 2020.
- Wang, H., Ge, S., Lipton, Z., and Xing, E. P. Learning robust global representations by penalizing local predictive power. In *Neural Information Processing Systems*, 2019.
- Wang, P., Yang, A., Men, R., Lin, J., Bai, S., Li, Z., Ma, J., Zhou, C., Zhou, J., and Yang, H. Unifying architectures, tasks, and modalities through a simple sequence-to-sequence learning framework. In *International Conference on Machine Learning*, 2022.
- Wang, X., Peng, Y., Lu, L., Lu, Z., Bagheri, M., and Summers, R. M. Chestx-ray8: Hospital-scale chest x-ray database and benchmarks on weakly-supervised classification and localization of common thorax diseases. In *Conference on Computer Vision and Pattern Recognition*, 2017.
- Wong, E., Santurkar, S., and Madry, A. Leveraging sparse linear layers for debuggable deep networks. In *International Conference on Machine Learning*, 2021.
- Wu, T., Ribeiro, M. T., Heer, J., and Weld, D. S. Errudite: Scalable, reproducible, and testable error analysis. In *Annual Conference of the Association for Computational Linguistics*, 2019.
- Xiao, K., Engstrom, L., Ilyas, A., and Madry, A. Noise or signal: The role of image backgrounds in object recognition. In *International Conference on Learning Representations*, 2021.
- Zhang, J., Wang, Y., Molino, P., Li, L., and Ebert, D. S. Manifold: A model-agnostic framework for interpretation and diagnosis of machine learning models. *IEEE transactions on visualization and computer graphics*, 25 (1):364–373, 2018.
- Zhang, M. and Ré, C. Contrastive adapters for foundation model group robustness. In *Neural Information Processing Systems*, 2022.
- Zhang, M., Sohoni, N. S., Zhang, H. R., Finn, C., and Ré, C. Correct-n-contrast: A contrastive approach for improving robustness to spurious correlations. In *International Conference on Machine Learning*, 2022.
- Zhao, J., Wang, T., Yatskar, M., Ordonez, V., and Chang, K.-W. Men also like shopping: Reducing gender bias amplification using corpus-level constraints. In *Conference on Empirical Methods in Natural Language Processing*, 2017.

A. Implementation details

A.1. B2T framework

We use ClipCap⁴ (Mokady et al., 2021) model trained on the Conceptual Captions (Sharma et al., 2018) dataset and decode captions without beam search. We concatenate the captions of mispredicted samples to create a corpus, then apply the YAKE⁵ (Campos et al., 2020) algorithm to extract the bias words. Here, we set the maximum n-gram size (i.e., length of keywords) as 3, the number of selected keywords as 20, and the deduplication threshold as 0.9, if not specified.

A.2. Datasets and classifiers for bias discovery

CelebA blond. CelebA (Liu et al., 2015) contains 19,867 validation images. We use the ResNet-50 classifiers released in the GDRO repository.⁶ Specifically, we use the ERM and GDRO models trained by a learning rate of 0.0001 and batch size of 128, which achieved accuracy for blond class of 85.96% and 93.68%, respectively.

Waterbirds. Waterbirds (Sagawa et al., 2020) contains 1,199 validation images. We use the ResNet-50 classifiers released in the GDRO repository. Specifically, we use ERM and GDRO models trained by a learning rate of 0.001 and batch size of 128. ERM achieved accuracy of 75.56% and 89.92%, and GDRO achieved 85.34% and 91.53% accuracies for waterbird and landbird classes, respectively.

Kaggle Face. Kaggle Face (Chauhan, 2020) contains 47,009 training and 11,649 validation images. We train a ResNet-18 classifier following the tutorial code.⁷ It achieved accuracy of 97.95% and 97.18% for female and male classes, respectively.

Dollar Street. We use the Dollar Street (Rojas et al., 2022) dataset released in the repository⁸, which contains the snapshot of the original web page on July 30th, 2019. We use the ResNet-50 classifier trained on ImageNet and evaluate it on Dollar Street. To do so, we convert the class names of Dollar Street to ImageNet names, as shown in Table 6.

Table 6: Conversion of class names from Dollar Street to ImageNet.

Dollar Street	ImageNet
books	book_jacket
computers	desktop_computer
cups	cup
diapers	diaper
dish_racks	plate_rack
dishwashers	dishwasher
necklaces	necklace
stoves	stove
tables_with_food	dining_table
toilet_paper	toilet_tissue
toilets	toilet_seat
wall_clocks	wall_clock
wardrobes	wardrobe
wheel_barrows	barrow
wrist_watches	digital_watch

ImageNet and variants. ImageNet (Deng et al., 2009) contains 50,000 validation images, 50 images per 1,000 classes. We use the ResNet-50 classifier trained on ImageNet with a classic training recipe (V1) from the PyTorch model hub⁹, which achieved 76.15% for vanilla ImageNet. We apply B2T for the hardest classes the classifier fails the most.

ImageNet-R (Hendrycks et al., 2021, rendition) contains 30,000 validation images of artistic versions of ImageNet classes. Samples of ImageNet-R belong to the 200-class subset of ImageNet, but we use the full 1,000 classes to infer classifiers. ImageNet-C (Hendrycks & Dietterich, 2019, corruption) contains corrupted versions of the ImageNet validation set. We use the snow and frost corruptions for demonstration. Each corrupted dataset contains 50,000 images corresponding to the

⁴https://github.com/rmokady/CLIP_prefix_caption

⁵<https://github.com/LIAAD/yake>

⁶https://github.com/kohpangwei/group_DRO

⁷<https://github.com/ndb796/Face-Gender-Classification-PyTorch>

⁸<https://github.com/greentfrapp/dollar-street-images>

⁹<https://pytorch.org/vision/stable/models.html>

vanilla ImageNet. We use the same ResNet-50 classifier trained on the vanilla ImageNet. This classifier achieved accuracy of 23.28%, 63.80%, and 67.01% for ImageNet-R, ImageNet-C snow, and ImageNet-C, respectively.

A.3. Debiasing methods

Inferring group labels. In Section 6.1, we introduce a method to infer the group labels of an image with CLIP zero-shot classifier by utilizing bias keywords inferred by B2T. Specifically, for CelebA dataset, our goal is to determine whether a training sample is of “man” group or not, and for Waterbirds dataset, our goal is to determine whether a training sample is in “land” or “water” background. For effective usage of zero-shot classifier, we use following tricks; first, we use general templates provided in official CLIP (Radford et al., 2021) ImageNet zero-shot classification.¹⁰ Also, we use dataset-wise template for better extraction of information. Lastly, we use various B2T keywords from Table 1 for group names to classify into group label. In general, the prompts are generated by "[general template]+[dataset-wise template]+[group name]", e.g., "a photo of a bird on a forest". In Table 7, we elaborate the complete list of prompt templates and group names we used. Here, we use CLIP ResNet-50 (He et al., 2016) model.

Table 7: Prompt design for inferring group labels.

Dataset	Dataset-wise Template	Group Name
CelebA	<ul style="list-style-type: none"> [group name] [group name] celebrity 	<ol style="list-style-type: none"> Male <ul style="list-style-type: none"> man male Non-male <ul style="list-style-type: none"> Empty string ""
Waterbirds	<ul style="list-style-type: none"> [group name] bird on [group name] bird on a [group name] bird and a [group name] fowl on [group name] fowl on a [group name] fowl and a [group name] 	<ol style="list-style-type: none"> Land background <ul style="list-style-type: none"> forest woods tree branch Water background <ul style="list-style-type: none"> ocean beach surfer boat dock water lake

Training debiased classifiers. For experiments in Section 6.2, we train B2T-GDRO following the practice of (Sagawa et al., 2020). For both datasets, we train ImageNet pre-trained ResNet-50 model with SGD optimizer of momentum 0.9. For CelebA dataset, we use batch size of 64, learning rate of $1e-5$, weight decay of 0.1, group adjustment of 0, and train for 50 epochs. For Waterbirds dataset, we use batch size of 128 and train for 300 epochs, and sweep the hyper-parameters {(learning rate, weight decay, group adjustment)} in the search space $\{(1e-3, 1e-4, 0), (1e-4, 0.1, 0), (1e-5, 1.0, 0), (1e-5, 1.0, 1), (1e-5, 1.0, 2), (1e-5, 1.0, 3), (1e-5, 1.0, 4), (1e-5, 1.0, 5)\}$ with validation worst-group accuracy. We report the test average and worst-group accuracies at the epoch with best validation worst-group accuracy.

¹⁰https://github.com/openai/CLIP/blob/main/notebooks/Prompt_Engineering_for_ImageNet.ipynb

Debiasing zero-shot classifiers. For the experiments in Section 6.3, we augment the prompt templates by appending a B2T inferred bias keywords at the suffix. We also use general templates provided for ImageNet zero-shot classification, and dataset-wise templates to further exploit the capability of CLIP zero-shot classifier. Table 8 lists the entire augmented templates with positive bias-likeness score B2T words. An example prompt for landbird class in Waterbirds dataset is "a photo of a landbird on the forest." We ensemble all possible combinations of prompts as same as inferring the group labels. We also use pre-trained CLIP with ResNet-50 (He et al., 2016) image encoder.

Table 8: Prompt design for bias-augmented zero-shot classification with positive bias-likeness score B2T words.

Dataset	Dataset-wise Template	Class Name
CelebA	<ul style="list-style-type: none"> • [class name] • [class name] man • [class name] player • [class name] person • [class name] artist • [class name] comedy • [class name] film • [class name] actor • [class name] face 	<ol style="list-style-type: none"> 1. Blond <ul style="list-style-type: none"> • non blond hair • celebrity of non blond hair 2. Non blond <ul style="list-style-type: none"> • blond hair • celebrity of blond hair
Waterbirds	<ul style="list-style-type: none"> • [class name] • [class name] on the forest • [class name] with woods • [class name] on a tree • [class name] on a branch • [class name] in the forest • [class name] on the tree • [class name] on the ocean • [class name] on a beach • [class name] on the lake • [class name] with a surfer • [class name] on the water • [class name] on a boat • [class name] on the dock • [class name] on the rocks • [class name] in the sunset • [class name] with a kite • [class name] on the sky • [class name] is on flight • [class name] is on flies 	<ol style="list-style-type: none"> 1. Landbird <ul style="list-style-type: none"> • landbird 2. Waterbird <ul style="list-style-type: none"> • waterbird

B. Comparison of different captioning models

We check if different captioning methods give consistent bias keywords for the B2T framework. To this end, we compare the bias words using ClipCap (Mokady et al., 2021), BLIP (Li et al., 2022) and OFA (Wang et al., 2022). We use “BLIP w/ ViT-B and CatFilt-L pretrained on 129M images” checkpoint for BLIP and “OFA-Huge” checkpoint for OFA.

Table 9 and Table 10 present the bias keywords for CelebA blond and Waterbirds using BLIP and OFA, respectively, following the setup of Table 1 using ClipCap. BLIP and OFA give similar words with ClipCap such as “bamboo” for waterbird and “ocean” for landbird, except OFA misses “man” for CelebA blond while BLIP catches. BLIP, OFA, and ClipCap also have some differences in selected words, e.g., BLIP finds a novel bias “long hair” for CelebA blond. Since different captioning models give different words, ensembling B2T for multiple captioning models would be helpful.

Table 9: Candidate of bias keywords using BLIP for CelebA and Waterbirds.

(a) CelebA blond (base acc.: 86.0)				(b) Waterbird (base acc.: 75.6)				(c) Landbird (base acc.: 89.9)			
	Score	Acc.	Bias		Score	Acc.	Bias		Score	Acc.	Bias
man	1.22	47.1	S	bamboo	2.89	40.0	S	ocean	3.41	64.7	S
long	0.34	88.9	S	forest	2.11	43.5	S	beach	2.83	69.3	S
long hair	0.05	60.5	M	woods	1.94	68.2	S	doberman	2.22	0.0	S
hair	0.02	91.5	M	tree	1.45	27.8	S	boat	2.16	70.4	S
woman with long	-0.69	89.5	-	flying	0.00	71.7	-	water	1.38	74.6	S
woman	-0.77	88.9	-	sitting	-0.19	66.7	-	lake	1.17	82.1	S
blonde	-1.34	95.2	-	top	-0.19	37.5	-	flying	-0.22	77.4	-
long blonde	-1.52	94.9	-	bird	-0.36	72.3	-	sitting	-0.78	93.7	-
blonde hair	-1.55	95.2	-	birds	-0.56	50.0	-	birds	-1.06	71.4	-
long blonde hair	-1.64	94.9	-	duck	-2.23	73.1	-	bird	-1.64	92.0	-

Table 10: Candidate of bias keywords using OFA for CelebA and Waterbirds.

(a) CelebA blond (base acc.: 86.0)				(b) Waterbird (base acc.: 75.6)				(c) Landbird (base acc.: 89.9)			
	Score	Acc.	Bias		Score	Acc.	Bias		Score	Acc.	Bias
titled actor	0.33	83.7	S	bamboo	2.89	35.3	S	beach	2.83	67.4	S
portrait	0.25	82.2	S	forest	2.11	48.1	S	water	1.38	50.0	S
person	0.17	83.6	S	tree	1.45	54.5	S	funny	0.16	78.9	S
portrait titled	0.16	83.3	S	reeds	0.73	28.6	S	animals	-0.14	85.7	-
artist	0.16	77.0	S	rain	0.05	33.3	S	flying	-0.22	84.8	-
actor	0.08	87.5	S	flying	0.00	75.8	-	animal	-0.53	78.9	-
portrait titled actor	0.05	84.3	S	species	-0.05	72.0	-	biological	-0.55	92.5	-
hair	0.02	91.0	-	biological	-0.28	71.4	-	species	-0.97	92.5	-
face	-0.02	91.2	-	bird	-0.36	65.2	-	birds	-1.06	90.9	-
smiles	-0.28	75.6	-	landing	-0.47	50.0	-	bird	-1.64	93.5	-

C. Full tables for B2T bias keywords

Table 11: Candidates of bias keywords for CelebA blond.

(a) Not blond (base acc.: 97.2)			
	Score	Acc.	Bias
model	0.50	96.9	S
favorite outfit	0.34	94.8	S
hair	0.33	94.4	M
love	0.17	96.7	M
style	0.14	94.7	S
premiere	0.11	98.0	S
clothing style	0.09	94.8	S
outfit	0.08	94.8	M
favorite	0.08	94.8	S
feet size	0.06	94.8	S
clothing	0.06	94.8	M
film	0.00	98.3	-
weight	-0.03	94.8	-
face	-0.05	97.3	-
feet	-0.06	94.8	-
size	-0.08	94.8	-
comedy	-0.25	96.5	-
person	-0.28	97.5	-
bob	-0.50	93.2	-
actor	-0.98	97.5	-

Table 12: Candidates of bias keywords for Kaggle Face.

(a) Female (base acc.: 98.0)				(b) Male (base acc.: 97.2)			
	Score	Acc.	Bias		Score	Acc.	Bias
shocked	0.52	94.4	S	woman	3.52	90.2	S
player	0.39	52.9	S	girl	3.45	50.9	S
named	0.25	94.0	S	actress	3.26	22.2	S
named person	0.25	35.7	M	girl's face	2.92	35.7	S
big	0.23	98.9	S	beauty	1.14	52.9	S
condition	0.23	94.5	M	love	0.64	97.0	S
found	0.22	95.7	M	eyes	0.61	96.7	S
person	0.22	96.8	M	face	0.52	95.3	S
love	-0.05	99.6	-	smile	0.42	96.7	S
face	-0.08	97.2	-	covered	0.30	86.1	S
fan	-0.13	97.3	-	movie	0.30	95.1	S
girl	-0.19	97.5	-	hair	0.27	95.4	S
hair	-0.20	99.5	-	person	0.27	97.4	M
dating person	-0.22	97.9	-	beautiful	0.17	66.7	S
movie	-0.22	97.8	-	found	0.17	95.8	M
girl face	-0.44	95.5	-	condition	0.11	95.5	M
woman	-0.45	96.8	-	named person	0.02	93.0	M
actor	-0.52	99.4	-	fan	0.02	98.3	S
actor as person	-0.59	97.1	-	actor as person	-0.75	95.6	-
smile	-0.63	98.3	-	actor	-1.34	98.0	-

Explaining Visual Biases as Words by Generating Captions

Table 13: Candidates of bias keywords for Dollar Street.

(a) Wardrobe (base acc.: 50.0)				(b) Stove (base acc.: 60.7)			
	Score	Acc.	Bias		Score	Acc.	Bias
cave	1.81	0.0	S	fire burns	1.28	0.0	S
man sleeps	1.53	0.0	S	fire	0.80	0.0	S
laundry	1.05	33.3	S	cat sits	0.27	0.0	S
man	0.67	0.0	S	fireplace	0.06	0.0	S
sleeps	0.30	0.0	S	cat	0.03	0.0	S
shed	-0.47	0.0	-	room	-0.17	0.0	-
living room	-0.53	0.0	-	small room	-0.47	0.0	-
clothes	-1.00	72.7	-	kitchen sink	-1.36	0.0	-
room	-1.22	58.3	-	kitchen	-1.59	50.0	-
laundry room	-1.59	0.0	-	stove	-1.64	61.5	-

(c) Plate rack (base acc.: 24.3)				(d) Toilet tissue (base acc.: 36.6)			
	Score	Acc.	Bias		Score	Acc.	Bias
bucket of water	1.06	5.9	S	bucket of water	3.09	0.0	S
bucket	0.80	3.8	S	bucket	2.11	0.0	S
water	0.77	3.0	S	water	1.56	2.1	S
sink	0.03	29.5	S	man	-0.45	40.0	-
full	-0.52	21.6	-	bathroom	-2.06	13.3	-
kitchen sink	-0.56	36.0	-	toilet	-2.78	73.3	-
kitchen	-1.13	32.3	-	paper	-3.22	60.0	-
dirty dishes	-1.38	8.3	-	toilet paper bag	-5.25	0.0	-
dishes	-1.41	25.0	-	toilet paper	-6.06	67.3	-
kitchen full	-1.45	20.0	-	toilet paper roll	-6.38	70.0	-

Table 14: Candidates of bias keywords for ImageNet.

(a) Toilet tissue (base acc.: 42.0)			(b) Beaker (base acc.: 44.0)		
	Score	Acc.		Score	Acc.
cat playing	0.92	0.0	beer	1.89	25.0
cat	0.61	0.0	close	1.06	50.0
playing	0.19	0.0	eggs	0.88	0.0
person	-0.59	57.1	glass bottle	0.45	33.3
paper bag	-0.64	0.0	bottle	0.44	62.5
woman	-0.70	40.0	poured	0.23	40.0
bathroom	-0.83	0.0	glass	0.03	45.8
paper cup	-1.55	0.0	water	0.03	50.0
paper	-1.81	75.0	glass of water	-0.20	40.0
toilet	-1.91	63.6	laboratory	-1.58	71.4

(c) Plastic bag (base acc.: 46.0)			(d) Notebook (base acc.: 36.0)		
	Score	Acc.		Score	Acc.
playing	1.61	0.0	office	1.78	16.7
streets	0.67	0.0	mess	1.64	0.0
street	0.61	33.3	motherboard removed	1.36	0.0
full of flowers	0.34	0.0	cat	1.19	0.0
man	0.16	42.9	removed	0.81	0.0
toddler	0.13	0.0	computer	0.80	50.0
person	-0.39	0.0	person	0.22	0.0
box	-0.95	25.0	good laptop	-0.20	0.0
plastic	-2.42	50.0	laptop keyboard	-0.25	0.0
plastic bag	-4.41	0.0	laptop	-0.27	34.4

Table 15: Candidates of bias keywords for ImageNet variants.

(a) ImageNet-R (base acc.: 23.3)			(b) ImageNet-C snow (base acc.: 63.8)			(c) ImageNet-C frost (base acc.: 67.0)		
	Score	Acc.		Score	Acc.		Score	Acc.
hand drawn illustration	3.44	1.6	snow falling	2.72	29.1	room	0.95	57.0
drawing	2.86	0.4	rain falling	2.31	25.9	window	0.75	51.2
vector illustration	2.83	0.5	rain drops falling	2.25	28.9	glass	0.72	51.2
white vector illustration	2.63	0.4	rain drops	2.00	30.2	water	0.52	66.9
illustration	2.03	0.5	rain	1.92	51.0	person playing	0.52	66.7
tattoo	1.86	0.7	snow	1.63	53.6	tree	0.31	73.1
white background vector	1.59	1.3	water drops	1.34	35.1	person	0.30	65.2
painting	1.25	1.0	falling	1.17	29.3	day	0.30	70.5
digital art	0.97	1.2	water	0.92	54.4	car	0.28	61.2
white background	0.81	5.3	day	0.45	72.1	dogs playing	0.35	55.6
step by step	0.81	0.4	car	0.39	68.0	make	0.20	71.4
art selected	0.63	1.1	person playing	0.39	64.0	man	0.09	52.0
art	0.59	0.6	person	0.20	64.6	close	0.08	73.2
digital art selected	0.50	1.1	playing	0.11	56.7	dog	0.00	70.7
pencil step	0.30	0.6	dog playing	0.09	54.7	dogs	-0.02	64.5
person	-0.36	25.1	man	0.03	44.5	biological	-0.11	87.1
vector	-0.41	0.6	dog	-0.05	68.0	black	-0.14	68.8
step	-0.45	0.7	dogs	-0.08	63.2	biological species	-0.17	87.1
dog	-0.53	27.2	black	-0.28	63.0	white	-0.23	68.5
white	-1.53	10.1	biological species	-0.30	85.3	species	-0.53	87.0

Table 16: Candidates of bias keywords for CelebA blond and Waterbirds using GDRO classifiers.

(a) CelebA blond (base acc.: 93.7)				(b) Waterbird (base acc.: 85.3)				(c) Landbird (base acc.: 91.6)			
	Score	Acc.	Bias		Score	Acc.	Bias		Score	Acc.	Bias
favorite outfit	0.53	95.2	S	bamboo forest	2.80	33.3	S	ocean	1.98	66.7	S
film	0.48	93.8	S	bamboo	2.13	33.3	S	surfer	1.55	50.0	S
love	0.36	94.6	S	forest	1.83	69.2	S	beach	1.30	90.7	S
outfit	0.34	95.2	S	woods	1.67	75.0	S	boat	1.14	85.0	S
portrait	0.31	79.1	S	tree	1.66	70.8	S	water	0.84	84.0	S
model	0.30	90.7	S	branch	1.23	66.7	S	dock	0.59	75.0	S
favorite	0.25	95.2	S	cat	0.97	0.0	S	fish	0.56	80.0	S
style	0.23	95.2	S	face	0.23	50.0	S	flight	0.19	62.5	S
clothing	0.16	95.8	S	bird	0.14	79.2	S	sky	0.14	85.7	S
clothing style	0.14	95.2	S	blue	0.14	66.7	S	person	-0.09	88.5	-
person	0.05	90.6	S	area	0.13	33.3	S	biological species	-0.17	93.4	-
weight	0.03	95.3	S	biological species	0.08	83.9	S	biological	-0.17	93.2	-
contestant	0.00	86.8	-	species	0.03	83.9	S	wild	-0.25	88.9	-
feet	-0.03	95.3	-	rock	-0.02	50.0	-	flies	-0.27	80.0	-
model and actress	-0.08	89.3	-	biological	-0.06	83.9	-	girl	-0.39	75.0	-
hair	-0.16	96.4	-	bird flying	-0.09	75.0	-	species in flight	-0.41	33.3	-
size	-0.20	95.3	-	pheasant	-0.09	0.0	-	species	-0.56	93.4	-
feet size	-0.25	95.3	-	bird in flight	-0.13	75.0	-	tree	-1.11	96.0	-
actress	-0.25	90.4	-	snow	-0.22	83.3	-	bird	-1.75	94.6	-
actor	-0.38	94.4	-	great bird	-0.28	0.0	-	bird stands	-1.92	0.0	-

D. Additional visual examples

Keyword	Man				Player				Hair			
Samples												
Actual	blond	blond	blond	blond	not blond	not blond	blond	blond	not blond	not blond	blond	blond
Pred.	not blond	not blond	not blond	not blond	blond	blond	not blond	not blond	not blond	not blond	not blond	not blond
Caption	actor is a man of many talents.	actor is a man of many faces.	the most important player in the history of hockey.	football player has been named the player of the year.	i'm not sure what this is, but i love the color of her hair.	actor - i love her hair like this.	i want my hair like this!.	i'm not a fan of the sun but i love her hair.				

Figure 7: Additional visual examples of CelebA.



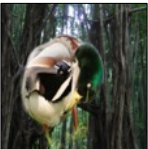
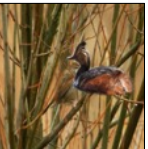




Keyword	Forest	Woods	Tree	Branch	Ocean	Beach	Surfer	Boat
Samples								
Actual	waterbird	waterbird	waterbird	waterbird	landbird	landbird	landbird	landbird
Pred.	landbird	landbird	landbird	landbird	waterbird	waterbird	waterbird	waterbird
Caption	the bird of the forest.	the bird of prey in the woods.	a bird in a tree.	a bird on a branch.	a parrot flies over the ocean.	a pelican is seen on the beach.	surfers surfing in the waves.	a yellow - billed stork in a boat.

Figure 8: Additional visual examples of Waterbirds.

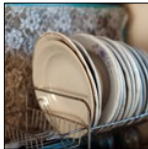



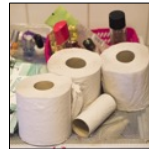


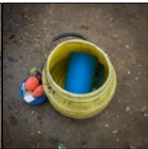
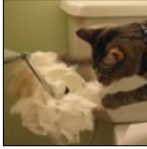





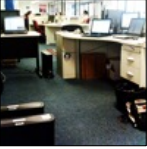
Keyword	-				Bucket			
Samples								
Actual	plate rack	plate rack	plate rack	plate rack	toilet tissue	toilet tissue	toilet tissue	toilet tissue
Pred.	plate rack	plate rack	oil filter	crock pot	toilet tissue	toilet tissue	bucket	bucket
Caption	a dishwasher and dryer in a kitchen.	a man is putting a lot of plates in the dishwasher.	a bucket of food is seen in a small kitchen.	a child's shoes and a bucket sit in a room in a refugee camp.	a stack of towels and a small pile of toilet paper.	a toilet seat with a toilet paper.	a bucket of water in a sink.	a bucket of water for the laundry.
Country (Income)	Bulgaria (\$654/month)	India (\$2499/month)	Haiti (\$107/month)	Liberia (\$48/month)	Sweden (\$1289/month)	Netherlands (\$3344/month)	Cambodia (\$307/month)	Nepal (\$85/month)

Figure 9: Visual examples of Dollar Street “plate rack” and “toilet tissue” classes.

Explaining Visual Biases as Words by Generating Captions

Keyword	Cat		Beer		Street		Office	
Samples								
Actual	toilet tissue	toilet tissue	beaker	beaker	plastic bag	plastic bag	notebook	notebook
Pred.	paper towel	paper towel	pop bottle	syringe	poncho	paddle	desk	laptop
Caption	cat playing with a paper cup.	cat playing with a paper bag.	the beer poured into the glass.	a glass of beer with a drop of water.	a homeless man begging on the streets.	actor reading a book on the street.	the office of person, who is now.	the laptop in my office.








Keyword	Snow		Forest		Grass		Red	
Samples								
Actual	Australian terrier	Australian terrier	hog	hog	terrapi	terrapi	mushroom	mushroom
Pred.	Tibetan terrier	Irish terrier	wild boar	wild boar	box turtle	mud turtle	agaric	agaric
Caption	person, a mix, playing in the snow.	dog in the snow, winter.	wild boar in the forest.	wild pigs in the forest.	a turtle on the grass.	turtle on the grass in the garden.	red mushroom in the forest.	red mushroom in the forest.

Figure 10: Additional visual examples of ImageNet classes.


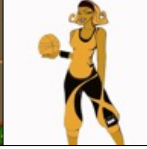
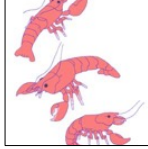




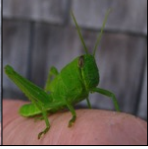
	(a) ImageNet-R				(b) ImageNet-C snow		(c) ImageNet-C frost	
Keyword	Illustration		Drawing		Snow		Window	
Samples								
Actual	African chameleon	basketball	American lobster	bee	Afghan hound	Afghan hound	grasshopper	grasshopper
Pred.	oscilloscope	knee pad	handkerchief	necklace	fountain	Afghan hound	African chameleon	grasshopper
Caption	vector illustration of a frog.	cartoon illustration of a basketball with an angry expression.	a drawing of a crab.	a drawing of a bee.	a horse in the snow.	person, the dog of the day.	a green chameleon on a window sill.	a green grasshopper on my finger.

Figure 11: Additional visual examples of ImageNet-R and ImageNet-C.

E. Additional comparison of different classifiers

We compare ViT-B trained by different methods: supervised model (ERM), multimodal learning - CLIP (Radford et al., 2021), and self-supervised learning - DINO (Caron et al., 2021) and MAE (He et al., 2022). We use the zero-shot classifier for CLIP, linear probing for DINO, and fine-tuned classifier for MAE. DINO and MAE are pre-trained and fine-tuned (or linear probed) in ImageNet. We extract 20 keywords but report the words with top 10 scores for brevity.

E.1. Multimodal learning: ERM vs. CLIP

Table 17 reports the bias keywords from ImageNet-R using ERM and CLIP models. ERM finds natural corruptions such as “illustration” and “drawing” with high bias-likeness scores. In contrast, CLIP finds other bias keywords such as “dog portrait” and has low bias-likeness scores, implying that CLIP suffers less from natural corruptions.

Table 17: Candidates of bias keywords from ViT-B, trained by ERM and CLIP.

(a) ERM (base acc.: 23.9)			(b) CLIP (base acc.: 74.4)		
	Score	Acc.		Score	Acc.
hand drawn illustration	3.45	1.2	dog portrait	0.64	59.0
drawing	2.88	0.4	tattoo	0.47	61.5
vector illustration	2.84	0.4	drawing	0.39	73.1
white vector illustration	2.66	1.2	dog	0.30	66.4
illustration	2.05	0.7	step by step	0.20	73.1
tattoo	1.84	1.0	art selected	0.19	68.8
white background vector	1.63	1.3	art	0.19	70.2
painting	1.25	1.2	painting	0.19	72.7
digital art	0.98	1.0	sketch	0.14	70.0
white background	0.83	5.4	illustration	0.13	73.9

E.2. Self-supervised learning: ERM vs. DINO vs. MAE

Table 18 reports the bias keywords from ImageNet-R using DINO and MAE models (ERM is in the table above). Self-supervised pre-training finds similar bias keywords with ERM, although their accuracies are on par. Namely, self-supervised learning does not fundamentally changes the model behaviors but improves the overall performance evenly.

Table 18: Candidates of bias keywords from ViT-B, trained by DINO and MAE.

(a) DINO (base acc.: 23.7)			(b) MAE (base acc.: 24.2)		
	Score	Acc.		Score	Acc.
hand drawn illustration	3.44	0.4	hand drawn illustration	3.47	0.4
drawing	2.84	0.5	drawing	2.89	0.7
vector illustration	2.81	0.8	vector illustration	2.88	0.6
white vector illustration	2.61	0.0	white vector illustration	2.69	0.8
illustration	2.05	0.7	illustration	2.06	0.5
tattoo	1.84	0.4	tattoo	1.88	0.7
white background vector	1.58	3.2	white background vector	1.66	0.6
painting	1.25	1.2	painting	1.25	1.2
digital art	0.97	1.2	digital art	0.98	1.1
white background	0.81	7.5	white background	0.86	5.4

F. Additional discussion on bias types

In this paper, we focus on the class-agnostic and class-specific versions of majority bias, which we call majority bias and spurious correlation, respectively. Here, we call it a “majority bias” in the sense that the classifier predicts the majority group well but fails for the minority group. By definition, we assume that the dataset has a subgroup (or subpopulation) that the classifier confuses, and thus our scope is limited to this “subgroup” type of bias. Here, we note that the definition of bias is more general, and many biases cannot be represented as majority bias. For example, data can contain multiple attributes that some attributes dominate the prediction, e.g., texture bias (Geirhos et al., 2019) for images or keyword bias (Moon et al., 2021) for texts. This bias appears in every sample and does not belong to the specific subgroup of the dataset.

We also note that we consider the “model” bias which is specific to the certain classifier; recall that ResNet and ViT give different bias keywords. Here, we use the terminology of “majority” for the ones that the model fails instead of the absolute number of samples in the dataset, which indicates the dataset bias. We claim that model bias is more informative for the users tackling the downstream task. Nevertheless, one may extend B2T to investigate the dataset bias by generating captions for all (not only the mispredicted) samples and finding the unique words in the captions.

Finally, we define the spurious correlation as the class-specific majority bias. This definition assumes that we are considering the model bias, as spurious correlation is a property of a specific classifier instead of the dataset bias. To be concrete, an attribute a is called spuriously correlated with a label y if it misleads the prediction of the classifier, i.e., misleadingly correlated but not causally related to the label. We call it the “majority bias” in the view of model prediction (instead of the absolute amount in a dataset) with a slight abuse of notation for a simple discussion progress.

G. Additional related works

Bias and fairness. Biases in the datasets and models are a long-lasting problem in machine learning (Torralba & Efros, 2011). While there are broad studies on various types of biases (Mehrabi et al., 2021), we focus on the majority (specifically, group type and model-specific) biases. Namely, our goal is to investigate the failure of the classifier that the model fails for some subgroups (or attributes) of the dataset. This failure is highly related to the fairness issue, as the model often underperforms for specific gender (Bolukbasi et al., 2016; Zhao et al., 2017; Hendricks et al., 2018) or race (Lee, 2018; Jalal et al., 2021). This failure is usually incurred by the imbalance in the dataset and further amplified during model training (Johnson & Khoshgoftaar, 2019). Imbalanced classification is highly related to the bias and fairness issue but developed independently following somewhat different setups (Kim et al., 2020b;a). We focus on the algorithmic solution for mitigating this bias or imbalance issue that strengthens the learning signal from minority samples (Rahimian & Mehrotra, 2019), but balancing the samples in the data collection stage is a more important and effective step (Roh et al., 2019).

Not only the fairness issue (or improving the worst-group accuracy), the bias is also highly related to the generalization performance, particularly when in the presence of distribution shifts (Muandet et al., 2013). Indeed, the ratio of majority and minority samples can vary, which may make the model prone to changing their constitution. This is also related to the shortcut in learning that the model overly relies on spurious features instead of core features (Geirhos et al., 2020). There are various types of shortcuts, such as texture bias (Geirhos et al., 2019), background bias (Xiao et al., 2021), and scene bias (Mo et al., 2021). We remark that our B2T framework could discover all these biases, e.g., “illustration” in ImageNet-R, “forest” and “ocean” in Waterbirds, and scene relation between “toilet tissue” and “cat” in ImageNet.

Bias discovery. Discovering biases (or explaining failures) of models has been widely studied, especially under the domains where features are interpretable, such as table (Zhang et al., 2018; Chung et al., 2019) or language (Wu et al., 2019; Ribeiro et al., 2020). However, analyzing biases of visual models is more challenging since the features are hard to interpret for humans. To this end, some prior works aim to label the visual features by crowdsourcing (Nushi et al., 2018; Plumb et al., 2022; Idrissi et al., 2022) or using a simulator (Leclerc et al., 2021). These approaches provide human-readable information, but require heavy annotation costs and may not be feasible for some visual domains.

Another line of work leverages interpretable machine learning (Molnar, 2020), specifically visualization techniques such as feature visualization (Olah et al., 2017; Engstrom et al., 2019) or saliency map (Selvaraju et al., 2017; Adebayo et al., 2018). They assume the images are composed of core and spurious features and visualize the features (or mask the salient regions) for human interpretation (Singla et al., 2021; Jain et al., 2022b). However, these approaches are hard to interpret since they only provide sample-wise visualization, not summarized insights of entire datasets or models. Thus, succeeding research tries to provide higher-level insights by analyzing the features with decision tree (Wong et al., 2021), ranking (Moayeri et al., 2022), and natural language description (Hernandez et al., 2022). Our work (B2T) is related to the final one called

MILAN. However, MILAN aims to interpret the visual neurons, unlike B2T focuses on understanding mispredicted images. In addition, B2T provides bias keywords that the users can easily understand and use for various applications.

Some works aim to identify the biased samples from hard-to-learn (potentially biased) samples in a similar spirit of B2T. Precisely, they detect the biased samples by simply retrieving the mispredicted samples (Liu et al., 2021), based on the training statistics (Nam et al., 2020), or clustering low-dimensional embeddings (Sohoni et al., 2020). B2T better determines the biased samples by leveraging the pre-trained vision-language models. Furthermore, B2T defines various bias groups based on their language explanations, applicable to complex real-world datasets with multiple biases.

We propose an alternative direction for bias discovery: use vision-language (captioning) models. A few recent works use vision-language models to discover biases (they call slices or model failures). Concretely, they define biased groups as the outliers in the embedding space of the visual encoder, estimated by a Gaussian mixture model (Eyuboglu et al., 2022) or support vector machine (Jain et al., 2022a). In contrast, we directly generate captions from images, which may contain more detailed information than the encoder embeddings. As a result, B2T can find multiple and fine-grained biases from descriptive captions. Recall that B2T only gives the suggestions of biases and the user makes the final decision, in contrast to the prior works finding the outliers first and then generating the description. It gives several advantages of B2T over prior works, e.g., B2T can effectively discover multiple potential biases without a repetitive finding of outliers.

Moreover, B2T has several technical and empirical contributions over the prior works. First, B2T can categorize the bias types as majority bias (e.g., “hair”) or spurious correlation (e.g., “man”), giving additional information for users. Using this information, we also train a debiased classifier by applying the group labels (for spurious correlation) inferred by B2T to GDRO (Sagawa et al., 2020) algorithm; unlike prior works only consider resolving the model failures (without such group information) by intervention. Moreover, we demonstrate various applications of B2T, discovering novel biases from real-world datasets such as a gender bias “player” and “shocked” for the female class in Kaggle Face, and analyzing the differences between classifiers, e.g., ViT understands the global context better than ResNet.

Debiasing classifiers. After identifying biases, a natural next step is to remove the biases from the classifiers. Numerous ideas were proposed under different names and assumptions, such as model debugging (Singla et al., 2022; Shah et al., 2022), model editing (Santurkar et al., 2021; Mitchell et al., 2022), and robust training (Wang et al., 2019; Arjovsky et al., 2019). They have different assumptions on biases (e.g., shortcuts like texture bias or minor groups for fairness) and training details (e.g., training from scratch or post-hoc fine-tuning for bias removal).

In this paper, we focus on distributionally robust optimization (Rahimian & Mehrotra, 2019, DRO), which aims to make the classifier robust to spurious correlations, i.e., improve the worst-group accuracy of minor groups. DRO is formulated as a minimax optimization $\min_f \max_a \ell(f, a)$ of minimizing the loss ℓ of the model f maximized over the groups (or attributes) a . Many training algorithms for DRO were developed, including bi-level optimization (Kim et al., 2019; Sagawa et al., 2020; Levy et al., 2020; Creager et al., 2021; Zhang et al., 2022) or disentangling core and spurious features (Lee et al., 2021). However, DRO requires group (or bias) labels a for every sample, demanding exhaustive annotation costs.

Thus, prior works attempted to reduce the labeling cost by estimating the bias labels in an unsupervised (Bahng et al., 2020; Nam et al., 2020; Sohoni et al., 2020; Liu et al., 2021; Bao & Barzilay, 2022) manner.¹¹ However, the unsupervised bias discovery methods are often inaccurate and not expandable for multiple biases, e.g., cannot distinguish “shocked” and “player” for gender classification. In contrast, B2T accurately infers the labels of multiple biases in a “zero-shot” manner, leveraging the power of vision-language models. Similar to the success of zero-shot image classification (Radford et al., 2021), we claim that the discovery of bias and sample-wise labeling should also be done in a zero-shot manner.

We remark that bias labeling in a zero-shot manner is not trivial. Zhang & Ré (2022) attempted to use CLIP for estimating the sample-wise bias labels (given that the “bias keyword” is known), but directly using group names might lead to inferior performance, e.g., see Table 3 for Waterbirds dataset. In contrast, B2T predicts the bias labels reasonably well, and using them for prompt tuning significantly improves the zero-shot classification without fine-tuning. Moreover, B2T finds the potential unknown biases, which can be more challenging than annotating sample-wise labels of the known bias.

Vision-language models. Vision-language models have shown remarkable success by pre-training from large-scale image-text pairs (Bommasani et al., 2021). They can be categorized into: joint embedding of image and text modalities (Radford et al., 2021; Lu et al., 2019), image-to-text (Desai & Johnson, 2021; Li et al., 2022), text-to-image (Ramesh et al., 2021), and hybrid (Wang et al., 2022) models. Our B2T framework can be applied to any type of model that can generate captions

¹¹Some works also consider semi-supervised (Sohoni et al., 2021; Nam et al., 2022a) setups.

(i.e., image-to-text) to predict the bias keywords, although we need a joint embedding model to determine the bias types further. Therefore, in our main experiments, we choose CLIP (Radford et al., 2021) as the default joint embedding model and ClipCap (Mokady et al., 2021) which is built upon CLIP embeddings, as the default image captioning model. For completeness, we also test other image captioning models such as BLIP (Li et al., 2022) and OFA (Wang et al., 2022) in Appendix B, and confirm that different image captioning models give reasonably consistent results.

H. Limitations and future works

Limitations. We discover the bias of image classifiers using pre-trained vision-language (e.g., CLIP, Radford et al. (2021)) and captioning (e.g., ClipCap, Mokady et al. (2021)) models. However, there is a potential risk that the vision-language model itself can be biased (Agarwal et al., 2021; Fang et al., 2022). Thus, the users should not completely trust the extracted captions, and the intervention of human juries is still essential for developing fair machine learning systems.

For instance, CLIP (and ClipCap) is mostly trained on natural images, and is less effective for specialized domains such as medical or satellite. To check this, we run B2T to ChestX-ray14 (Wang et al., 2017) and FMoW (Christie et al., 2018, functional map of the world) datasets. We use the classifiers publicly released in ChexNet¹² (Rajpurkar et al., 2017) and WILDS¹³ (Koh et al., 2021) codebases. We use the ERM classifier seed 0 for FMoW. Figure 12 visualizes the images and corresponding captions. ClipCap generates non-sense captions such as “broken nose” for chest images or trivial captions such as “city from air” for air-view images. Here, one needs to train a specialized captioning model to apply B2T.



	(a) ChestX-14ray		(b) FMoW	
Samples				
Actual	no disease	disease	crop field	Parking lot or garage
Pred.	disease	no disease	debris or rubble	place of worship
Caption	a picture of a patient with a broken nose.	a picture of a woman with a broken neck.	a small village in the middle of the desert.	a city from the air.

Figure 12: Visual examples of (a) ChestX-ray14 and (b) FMoW datasets.

Ethical concerns. Bias and fairness research intrinsically has potential negative social impacts. We remark that B2T does not aim to *fully automate* the procedure of discovering biases but *assist* humans to make a decision based on the suggested candidates of bias keywords. We leave the final judgment to the users, who should also be monitored by a cross-verification system. We used some sensitive examples of gender and geographic biases. We emphasize that our purpose is to alert and prevent potential risks in real-world datasets, which are publicly accessible from Kaggle or Dollar Street websites.

Future works. We discussed various applications of B2T, including discovering unknown biases in datasets, analyzing behaviors of classifiers, and debiasing zero-shot and full-shot classifiers. Applying B2T to more challenging real-world problems would be an exciting and impactful future direction. Also, one can extend B2T for creating a fairness or bias benchmark using the B2T bias keywords or designing a robust classifier by comparing models with B2T.

In addition, the concept of B2T can be extended to generative models by analyzing the underrepresented (or mode collapsed) samples (Nam et al., 2022b). To this end, one can infer the bias keywords from the low-density samples instead of the wrong ones from the classifier. Specifically, one can collect the samples with a low likelihood for diffusion model (Song et al., 2021), VAE (Vahdat & Kautz, 2020), normalizing flow (Kingma & Dhariwal, 2018), and autoregressive model (Esser et al., 2021), and the samples with a high real/fake density ratio (Mo et al., 2019) for GAN (Karras et al., 2021).

¹²<https://github.com/arnoweng/ChexNet>

¹³<https://worksheets.codalab.org/worksheets/0xa96b8749679944a5b4e4e7cf0ae61dc9>